CHAPTER 7

MECHANICAL AND THERMAL PROPERTIES OF SISAL/COTTON FIBRES REINFORCED POLYPROPYLENE HYBRID NANOCOMPOSITES

7.1 INTRODUCTION

This Chapter discusses the mechanical, thermal properties and morphological behaviour of sisal/cotton fibres reinforced Polypropylene hybrid nanocomposites.

7.2 MATERIALS AND METHODS

These have already been given in Chapter 3.

7.3 RESULTS AND DISCUSSION

7.3.1 Mechanical Properties

The effect of nano clay on tensile strength of cotton and sisal Polypropylene composites is shown in Table 7.1 and Break strain is shown in Table 7.2. The various compositions were compared with neat cotton and sisal Polypropylene composites.

7.3.2 Tensile Properties of Nano Composites

The tensile properties of various compositions of fibre reinforced Polypropylene nano composites are shown in the Table 7.1

Table 7.1 Tensile properties of CSFP nano composites

Sample Type (wt %)	Tensile strength (MPa)	Tensile modulus (GPa)	Flexural strength (MPa)	Flexural modulus (MPa)	Impact strength (J/m)
0	23.18±0.8	1500±3.5	47.75±0.8	1500±5.6	85.64±0.92
1	24.22±0.6	1530±2.3	48.22±0.6	1700±4.7	86.32±0.88
3	26.638±0.67	1570.4±4.2	58.148±0.77	7416±4.5	89.55±0.66
5	24.012±0.84	1550.710±3.9	49.158±0.65	3136.46±3.3	87.69±0.76
7	23.24±0.55	1048.26±2.2	38.455±0.55	2972.45±3.6	80.08±0.54

The variation of the mechanical properties of the nanocomposite as a function of clay modification and loading in presence of compatibilizer is represented in Table 7.1 . It is evident that there is an increase in tensile, flexural, and impact properties with a maximum, corresponding to the samples containing 3 wt% of clay. The tensile strength, modulus of elasticity, lexural strength, flexural modulus, and impact strength showed an improvement 26.638, 1570.4, 49.158, 7416 and 89.55 respectively as compared to the 30% . However, the mechanical strength decreased with the increase in clay loading to 5 and 7%. Since, the nanocomposite prepared using 3wt% of clay showed optimum mechanical performance, this composition has been retained for further investigation using the clays. The test results reported in Table 7.1 showed that incorporation of clay within 30% CSFP matrix resulted in marginal improvement in the mechanical properties which is primarily due to incompatibility between the matrix polymer and the nanoclay. This increment in tensile strength and modulus is primarily attributed to the reinforcing characteristics of dispersed nanolayers with high aspect ratio. It is expected that, the macromolecules contacted to the solid silica would have different responses from those containing the matrix

because of the mechanical displacement resulting from elongation, which is responsible for the increased modulus of the nanocomposites (Ji et al 2002). The increase in flexural strength and modulus is attributed to the high stiffness of nanolayers. Similarly the increment in impact strength of the nanocomposites may be due to the inter diffusion of polymer matrix through the interlayer galleries of the montmorillonite. An optimum increase in the mechanical properties of PP/Cloisite 25A nanocomposite is mainly due to maximum exfoliation of clay galleries and uniform dispersion of the clay platelets within the polymer matrix, as compared with others. Similar observations were also reported for other polymer/clay nanocomposites by Kojima et al and Messersmeith et al. Furthermore, the presence of long alkyl tallow units in the Cloisite 25A renders.

Table 7.2 Breaking strain and maximum load of hybrid nano composites

Sample Type (wt%)	Break strain (%)	Maximum load (N)
0	1.013	102.29
1	1.010	37.12
3	1.717	40.70
5	1.784	97.22
7	0.861	52.31

Random packing arrangement of the chains within the clay galleries (Kurokawa 1996) The mechanical findings are in agreement with the morphological investigations. The decreased strength and toughness of nanocomposites at higher nanomer loading might be due to core distribution of nanoparticle cluster present in the resulted hybrids. The decrease in impact strength is attributed to the detrimental effect of nanomer agglomerate due to

nonuniform dispersion of clay nanolayers in the polymer matrix (Chow et al 2004).

7.4 WATER ABSORPTION BEHAVIOUR

From the water absorption test, found in Table 7.3 it has been observed that the PP nano composites absorb water more than that of virgin PP due the presence of natural fibres along with clay.

Table 7.3 Water absorption test results

S.No	Sample Type (wt%)	Percentage of water absorption (%)
1	0	1.25
2	1	1.35
3	3	0.74
4	5	0.167
5	7	2.92

7.5 SEM ANALYSIS

SEM micrographs of 3% and 5% mer - CSFP nano composites are shown in the Figures 7.1 and 7.2 Due to the addition of MAPP the interfacial bonding of cotton and sisal fibre with PP was very good. SEM micrograph also shows that there is a better dispersion of fibres in the PP matrix. Figures 7.1 and 7.2 shows presence of nanoclay with a dimension of 150.1 nm and better dispersion of the same.

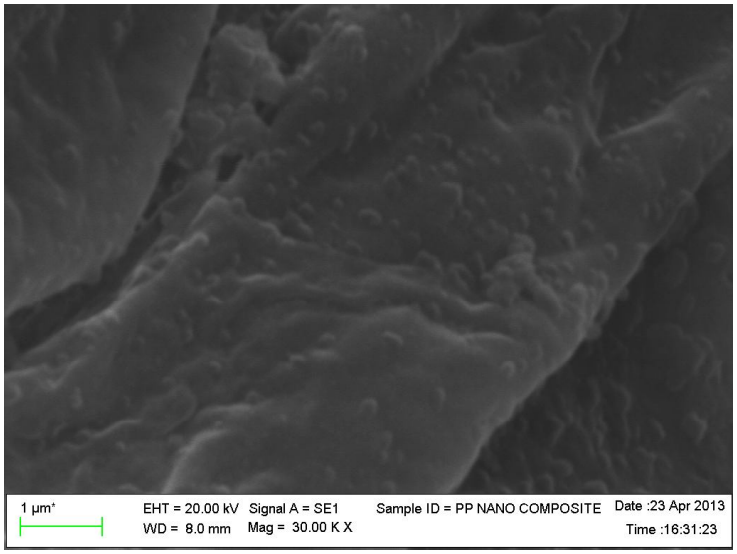

Figure 7.1 SEM image of 3% of nanoclay

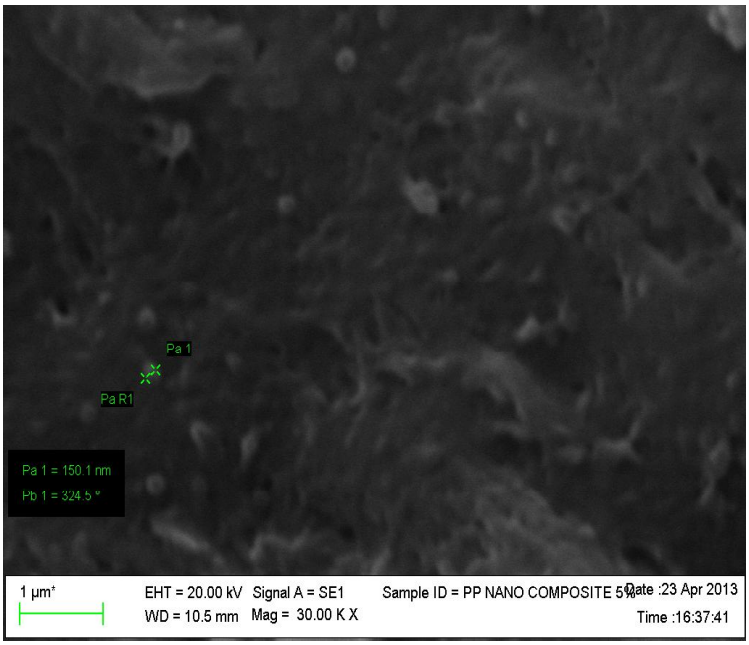

Figure 7.2 SEM image of 5% of nanoclay

7.6 THERMAL PROPERTIES

7.6 .1 Crystallization And Melting Behavior

The crystallization behaviour of virgin PP and the nanocomposites are reported in Figures 7.3 and 7.4 and Table 7.4.

Table 7.4 Crystallization and melting behaviour of nanocomposites

Sample Type (wt %)	T_m (° C)	T_c (°C)	Enthalpy of melting J/g	X_c (%)
0	167.2	101.4	78.69	32.78
1	169.3	103.2	79.1	32.9
3	175.3	107.4	79.8	33.25
5	171	108.1	60.7	25.29
7	168.5	109.8	71.72	29.88

The crystallization temperature (Tc) of the 30% CSFPP (167.2° C) increase significantly with the addition of nanoclays upto 3% and then decreases. This increase indicates the nucleating effect of the nanoclays in the crystallization of CSFP. Many studies have shown nucleating effect of nanoclays for different polymers (Kodgire 2001; Maiti 2002). This effect can be used to enhance the mechanical and thermal properties of the polymer.

The degree of crystallinity (Xc) calculated by using the following equation also varied with

$$X_c = (\Delta H_m / \Delta H^*)100 \qquad (7.1)$$

where ΔH_m and ΔH are the heat of fusion of nanocomposites and PP with 100% crystallinity. According to the literature (Van Krevelen 1997), ΔH of

100%crystal and PP is estimated to be 240 J/g. PP/Cloisite 25A nanocomposites had higher Xc than pure CSFP, while others had lower Xc than pure PP. Figure 7.3 and 7.4 and Table 7.4 show the cooling and melting curves and values of Tm of the different nanocomposites. Similar experimental facts have also been described by Lei and co-workers (Lei et al 2006) with the variation in clay types on the processing and properties of PP nanocomposites.

7.6.2 Thermal Stability

The thermal stability of CSFP and PP/clay nanocomposites are studied by TGA analysis as shown in Table 7.5. From the observation it is clear that (Figure 7.5). Crystallization Cooling scans of (a) CSFP nanocomposites containing 3wt% Melting and Crystallization behaviour of virgin CSFP the thermal stability of the base polymer increased with nanomer loading from the initial decomposition temperature of 458.8°C to 465.1°C . The increase in thermal stability of nanocomposites is attributed to the organic/inorganic interaction between the polymer and nanoclays (Doth and Cho 1998). By comparing the thermal stability and weight loss with the nanocomposites in presence of MAPP, it is observed that the weight loss at final decomposition temperature is higher for the compatibilized nanocomposites. The enhanced thermal stability is attributed to the strong interaction of base polymer and clay surface through chemical linkage between compatibilizer and nanoclays, which in term mediate the surface polarity of the clay and the clay – polymer interface. The organoclay delays volatization of the products generated at the temperature of carbon–carbon bond scission of the polymer matrix.

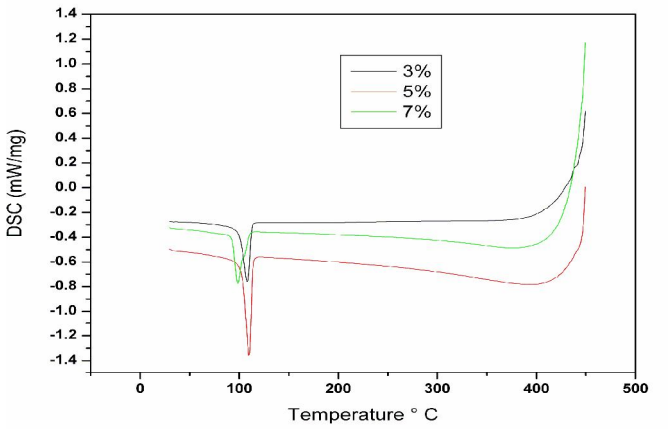

Figure 7.3 cooling curves of CSFP nanocomposites(exo 1.1 ↓)

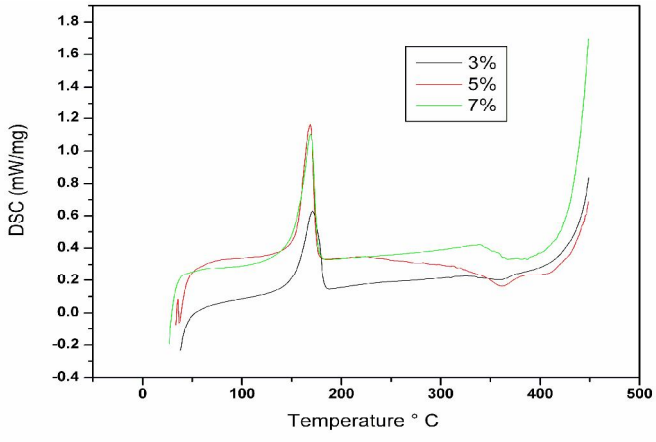

Figure 7.4 Heating curve of CSFP nanocomposites (exo 1.1 ↓)

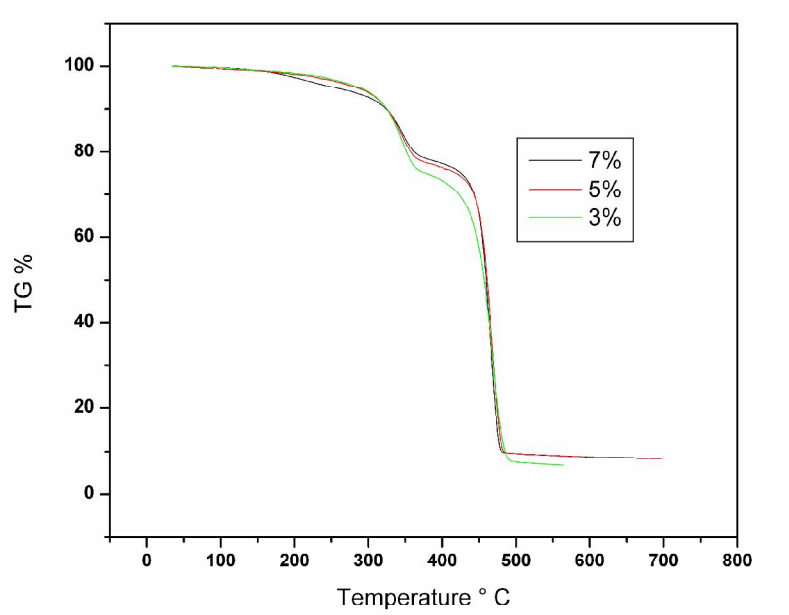

Figure 7.5 TGA of CSFP nanocomposites

Table 7.5 Thermal stability of CSFP hybrid nano composites

Sample Type (wt %)	Onset Temperature (T_1 °C)	Peak Temperature(T_{max} °C)		Weight loss (%) at peak second temperature	Residue after 600 ° C
		First peak	Second peak		
0	368.96	No peak	458.8	87.36	1.77
1	290	340	460.1	63.2	2.8
3	290	347.8	468.7	62.93	6.68
5	260	347.1	466.3	66.64	8.23
7	240	349.6	465.1	68.6	8.43

7.7 X-RAY DIFFRACTION (XRD)

The changes in the interlayer distance of clay can generally be elucidated using XRD. A shift to lower angles in the peak represents the formation of an intercalated structure (Parija 2004), where as the

disappearance of the peak signals the potential existence of an exfoliated structure. Figures 7.6 and 7.7 display the wide angle X-ray diffraction patterns of all the nano composites.

X-ray diffraction patterns of 30% mer- CSFP and compatibilizer nanocomposites prepared using Cloisite 25A, nanoclay at 3 wt% clay loading is illustrated in Figure 7.6. Cloisite 25A nanocomposites did not exhibit any peak within the experimental range, which indicated exfoliated structure. It also demonstrated superior composite performance as discussed under mechanical & thermal properties. Structure of clay breaks due to pressure exhorted by the intercalated polymer leaving behind exfoliated composition. This leads to the disappearance of the peak in the low angle XRD spectra as in Figure 7.7.

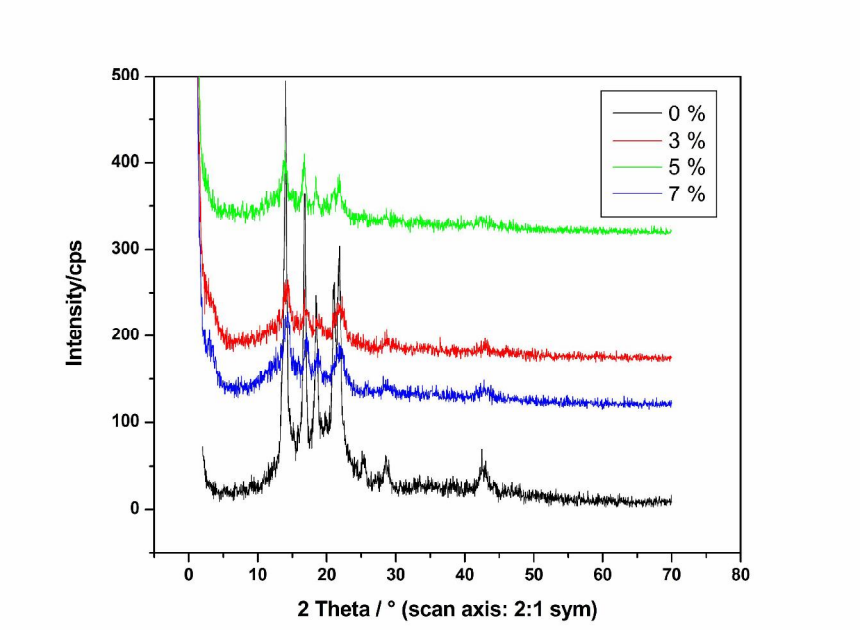

Figure 7.6 XRD of CSFP nanocomposites

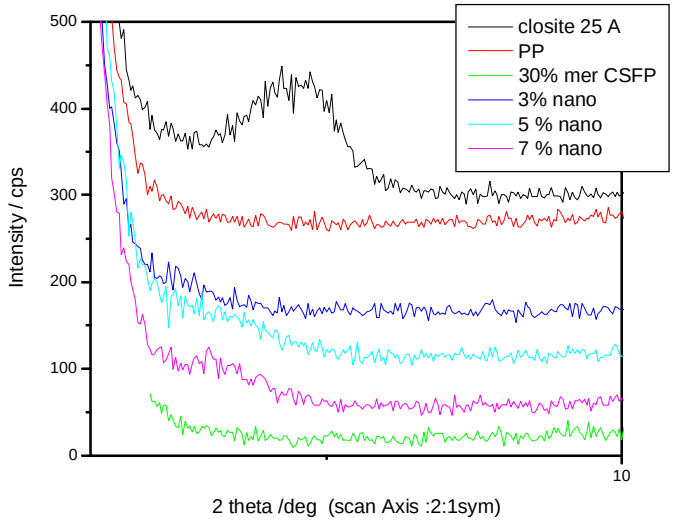

Figure 7.7 XRD of CSFP nanocomposites in lower angle

7.8 CONCLUSION

MAPP nanocomposites were successfully prepared by employing melt intercalation technique. The comparative performance of the nanocomposites were studied. The WAXD patterns showed that the addition of clay improved the clay dispersion in the CSFP matrix in presence of compatibilizer. Among all composition 3% of nanoclays used in this study, have shown better mechanical properties than others. Further good toughness and stiffness were coexistant in the CSFP/clay nanocomposites compatibilized with 2 wt% of MAPP. All the composition of clay has demonstrated the apparent nucleating effect because the crystallization took place at higher temperature upon cooling. The crystallization Temperature (°C) is also affected by the intercalants characteristics. TGA thermographs showed higher thermal stability in case of the nanocomposites. This is significant as most of the commercial applications of layered silicate nanocomposites will be commercially viable if they are cost competitive with regular additive approaches to modify polymer properties.